SUPPORTING INFORMATION

B Cell-Intrinsic MyD88 and BCR Signaling Promote NASH by Driving Hepatic Inflammation and Fibrosis

Fanta Barrow, Saad Khan, Gavin Fredrickson, Haiguang Wang, Katrina Dietsche, Preethy Parthiban, Sacha Robert, Thomas Kaiser, Shawn Winer, Adam Herman, Oyedele Adeyi, Marialena Mouzaki, Alexander Khoruts, Kristin A. Hogquist, Christopher Staley, Daniel A. Winer, and Xavier S. Revelo.

Contact Information:
Xavier S. Revelo, Ph.D.
Cancer & Cardiovascular Research Building
2231 6th St SE
Minneapolis, MN 55455
Phone: +1 (612) 301-7688
Email: xrevelo@umn.edu

SUPPLEMENTARY EXPERIMENTAL PROCEDURES

Experimental Animals

Heterozygous mice were crossed to generate WT and μMT or Nur77^{GFP} littermates. Cd19^{cre} and MyD88^{fl} were crossbred to generate Cd19^{cre}MyD88$^{fl/fl}$ (B-MYD) and CD19$^{-/-}$ MyD88$^{fl/(-/fl)}$ (WT) littermate controls. All mice were male, age-matched, and housed in a standard pathogen-free environment.

Metabolic Studies

Glucose tolerance tests (GTT), insulin tolerance tests (ITT), and pyruvate tolerance tests (PTT) were performed as previously described (1). Liver triglyceride content was measured using a colorimetric assay kit (Cayman Chemical). Serum ALT and AST were assessed by the Marshfield Laboratories (Marshfield Clinic Health System).

Immune Cell Isolation and Characterization

Immune cells were isolated from perfused livers using density gradient centrifugation (2). Splenic, adipose tissue, and colon lamina propria immune cells were harvested as previously described (3). In cytometry by time-of-flight (CyTOF) analysis, cells were stained with 0.5 μg of metal-conjugated primary antibodies (Fluidigm) for 30 mins at 4^{o}C. Data was acquired on a CyTOF2 (DVS Sciences) and analyzed using Cytobank. For flow cytometry, cells were incubated with fluorophore-conjugated primary antibodies for 30 mins at 4^{o}C. Flow cytometry data were acquired on a BD Fortessa X-20 (BD Biosciences) and analyzed using Flowjo software. Antibody information is provided in **Table S4**.

Detection of Intracellular Cytokines and ELISA

For phorbol-myristate-acetate (PMA) stimulation, $1x10^6$ immune cells were stimulated with 1X PMA with protein transport inhibitor (eBioscience) for 5 hours. For TLR stimulations, cells were treated with 5 µg/mL of LPS (eBioscience), 5 µM of ODN1826 (Invivogen), or 150 ng/mL of Pam3CSK4 (Invivogen) for 24 hours with a protein transport inhibitor (eBioscience) added for the last 12 hrs.

For ELISA measurement of cytokines, B cells (87% pure) were isolated from immune cell suspensions using the EasySep Pan-B cell isolation kit (StemCell Technologies). Macrophages (98% pure), and neutrophils (85% pure) were labeled using anti-F4/80 and -Ly6G microbeads and purified using LS columns and a MACS separator (Miltenyi Biotech). Two hundred thousand cells were stimulated with 5 µg/mL of LPS for 5 days. The supernatant was collected and the amounts of tumor necrosis factor (TNF)α and interleukin (IL)-6 were quantified using the ELISA MAX kits (Biolegend).

Single-cell RNA sequencing

Cells from each sample were individually incubated with 0.5 µg of Totalseq-A hashtag antibodies (Biolegend) for 30mins at 4C to allow for downstream multiplexing of samples. Samples were then combined and loaded into 2 capture ports of a 10X Genomics chip at a concentration of 1,500 cells/µl. Separate libraries were created for gene expression and HTO (cell hashing) and sequenced using a Novaseq S4 chip (2 x 150bp PE). Feature quantification was performed using cellranger (version 3.0, 10X Genomics). All subsequent analyses were performed using Seurat 3.1.1 (4). After sample demultiplexing of hashtag barcodes, we retained single cells and normalized within each pool using the

sctransform method in Seurat (4). Visualization of different clusters was enabled using Uniform Manifold Approximation and Projection (UMAP) dimensional reduction (5). The identity of cell types in these clusters was determined using SingleR (6). Differential expression testing was performed using the default Wilcoxon rank-sum test.

Bulk RNA Sequencing

Total RNA was extracted from purified B cells using the RNeasy Plus Mini kit (Qiagen). Illumina sequencing libraries were created using the SMARTer Stranded RNA Pico Mammalian V2 kit (Takara Bio) and sequenced on a single lane in a NextSeq 550 instrument (Illumina) using the 75bp paired-end Mid Output Mode. Differential gene expression analysis was performed using edgeR (Bioconductor) and pathway analysis was completed using Ingenuity Pathway Analysis (IPA, Qiagen).

Quantitative Real Time-PCR

Total RNA was extracted from livers using the RNeasy Plus Mini kit (Qiagen) and cDNA was prepped using the iScript cDNA Synthesis kit (Bio-Rad). Gene expression was normalized to GAPDH and changes in gene expression were calculated with the $2^{(-\Delta\Delta CT)}$ method. Primers are listed in **Table S1**.

Histology

Liver sections fixed in 10% formalin were assessed for steatosis and fibrosis by Masson's trichrome and hematoxylin & eosin (H&E) staining by the Biorepository & Laboratory Services at the University of Minnesota. The NAFLD activity score (NAS) was used to

semi-quantitively evaluate histological features (7). A liver pathologist performed the blinded histological evaluation. The collagen volume fraction in Masson's trichrome staining images on 10X resolution was quantified using the Weka Trainable Segmentation plugin in FIJI software (ImageJ, version 1.52p). Approximately ten different sections per histological slice were analyzed. Blue staining of collagen deposition was segmented from the other colors using the plugin classifier. Images were then converted to RGB color and the segmented color of collagen was isolated using color thresholding. The percent area positive for collagen was calculated for each section using binary processing.

Anti-CD20 Treatment

Mice were fed the HFHC diet for 6 weeks followed by intraperitoneal injections every 3 weeks with 250 µg of monoclonal anti-CD20 antibody (clone 5D2) or GP120 isotype control. Mice were euthanized 15 weeks after diet initiation.

Adoptive Transfer

Splenic and hepatic B cells were isolated from WT mice fed the HFHC diet for 15 weeks. 1×10^6 B cells from either the liver or spleen were intraperitoneally injected into 11-week HFHC-fed µMT recipient mice. Animals were euthanized 4 weeks after adoptive transfer.

Human Specimens

Fecal samples were collected from patients with no infectious risk or antibiotic use in the last 3 months and processed within 2 hours of collection and screened for routine enteric pathogens, as previously described (8). For the assessment of B cells in the human liver,

we used specimens from a cohort of 18 NAFLD patients with varying degrees of disease followed at the University Health Network (2). Liver specimens were stained for hematoxylin and anti-human CD19 (Thermofischer scientific, clone LE-CD19), given a NAFLD Activity Score (NAS) followed by $CD19^+$ B cells enumeration per high power field (HPF = 0.237 mm^2). Livers with a NAS ≥ 4 were considered to have progressed to NASH (9). Human liver specimens were obtained with approval by the Research Ethics Board at the University Health Network.

Fecal Microbiota Transplantation

DNA was extracted from mouse and human stool samples, followed by amplification of the V4 hypervariable regions of the 16S rRNA gene and sequencing on the Illumina MiSeq platform. Reads were processed and sequences were aligned against the SILVA database. Taxonomy was assigned using the Ribosomal Database Project. The alpha diversity of microbial communities was determined using Shannon indices and SourceTracker software was used to determine the similarities between the recipient and donor operational taxonomic units (8).

SUPPLEMENTARY RESULTS

B Cells Accumulate in the Livers of a Cohort of NAFLD Patients

We assesed CD19^{+} B cells in liver biopsies from a cohort of patients with varying degrees of NAFLD. We detected B cells in liver specimens of the NASH patients with a positive correlation between NAS and B cell infiltration in the hepatic lobular and portal areas. Of the 18 patient liver biopsies assessed, 7 presented NASH as defined by a NAS ≥ 4 **(Fig. A).** In agreement with a previous report (10), we detected B cells in liver specimens of the NASH patients **(Fig. B)** with a positive correlation between NAS and B cell infiltration in the hepatic lobular and portal areas **(Fig. C)**. Accordingly, the patients that presented NASH (NAS ≥ 4) had increased lobular and portal B cells compared with those with fatty liver alone **(Fig. D).** These findings suggested that B cell accumulation was progressive and associated with the development of NASH in a cohort of patients.

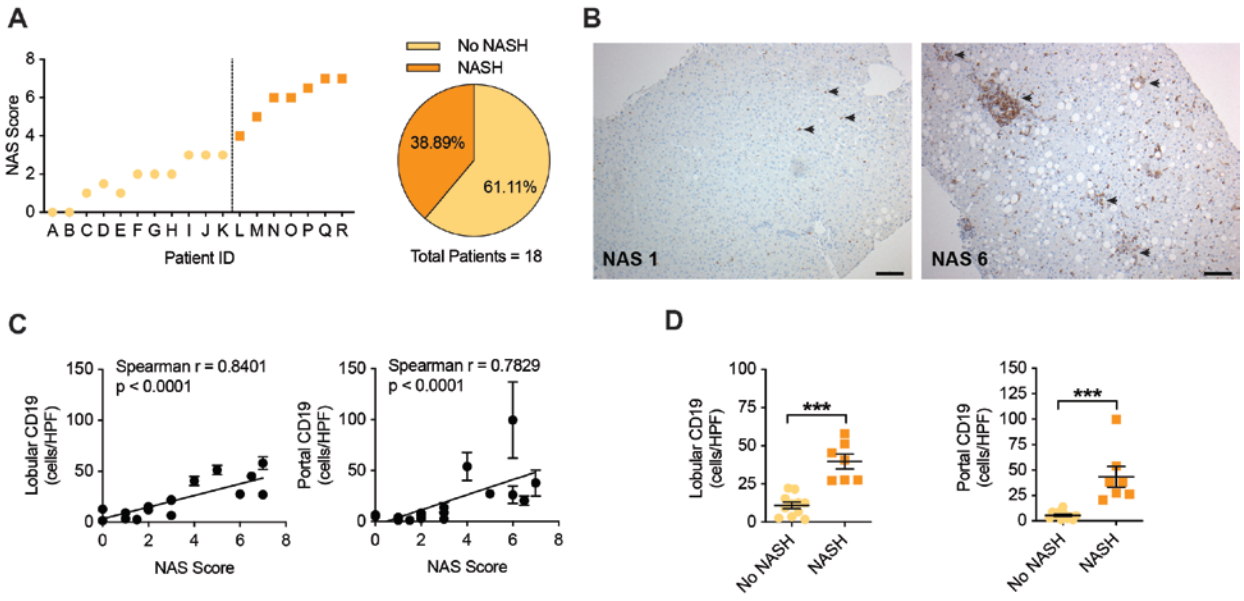

(**A**) NAS scores of patients in the NAFLD cohort (n =18).

(**B**) Representative immunohistochemical staining of human liver biopsies (n = 18) given NAS scores and stained for CD19 (brown) indicated by arrows. Magnification, 200X. Scale bar, 100μm.

(**C**) Correlative analysis between NAS score and lobular (left) or portal tract (right) $CD19^+$ B cells per high power field (HPF, 0.237 mm^2) of human liver biopsies (n = 18) as in (A). Spearman r values and p values denoting statistical significance are indicated in the figure graphs.

(**D**) Number of lobular (left) and portal tract (right) $CD19^+$ B cells in No NASH (n = 11) and NASH (n = 7) patients.

SUPPLEMENTARY FIGURES

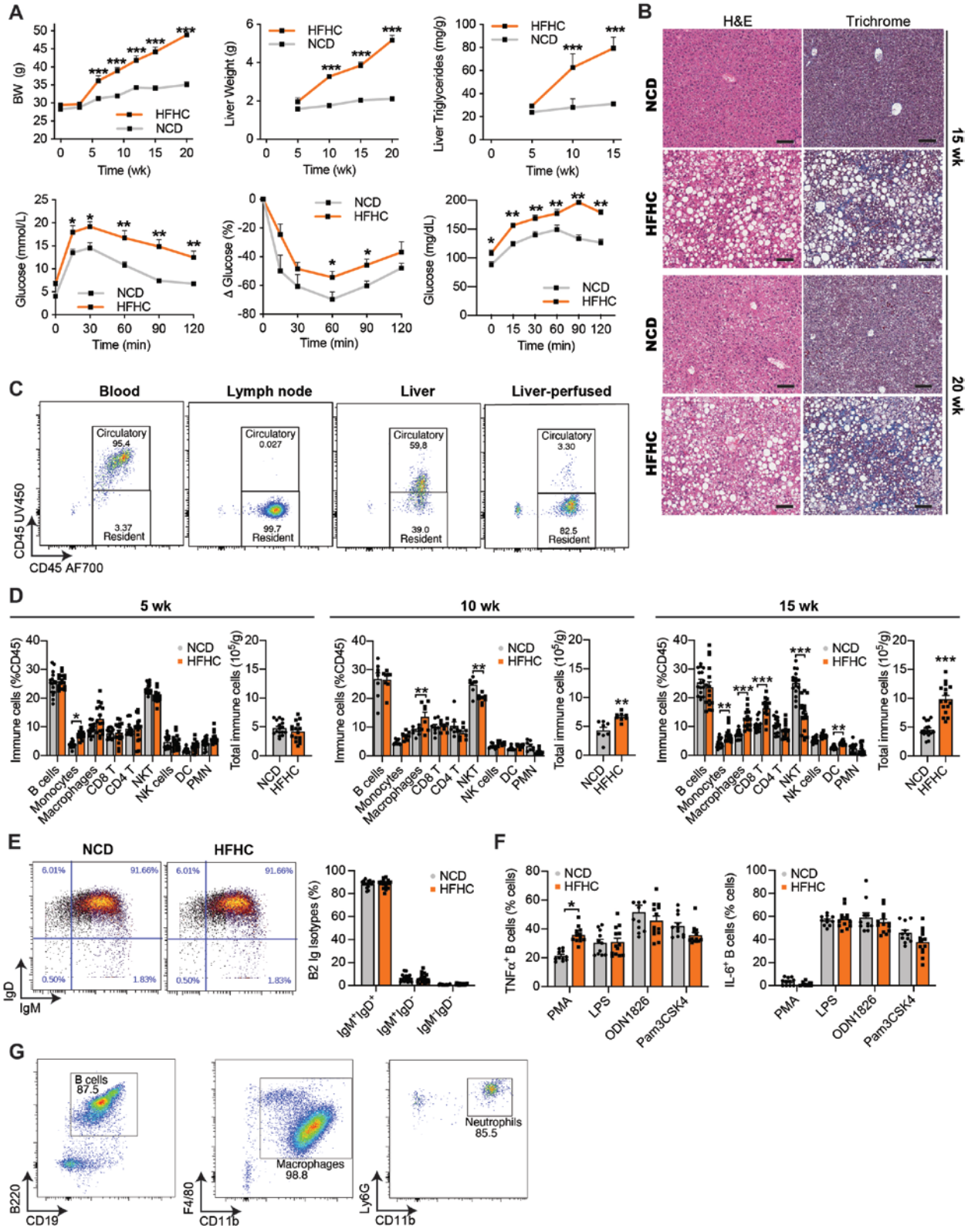

Supplementary Fig. 1 (Related to Fig. 1). Additional Data for WT mice fed the NASH-Inducing Diet and Intrahepatic B Cell Phenotype

(**A-B**) WT mice were fed either a normal control diet (NCD) or the NASH-inducing, high-fat, high-carbohydrate (HFHC) diet for up to 20 weeks.

(**A**) Body weights (upper left, n = 6 mice per group), liver weights (upper middle, n = 7-12 mice per group), liver triglyceride content (upper right, n = 5-6 mice per group), glucose tolerance test (lower left, n = 5 mice per group), insulin tolerance test (lower middle, n = 4-5 mice per group), and pyruvate tolerance test (lower right, n = 8 mice per group) after 15 weeks of dietary treatment.

(**B**) Representative H&E and trichrome liver stains (200X magnification, Scale bar, 100 μm; n = 3 mice per stain)

(**C**) Flow cytometry plots showing circulatory and resident $CD45^+$ immune cells in the blood, lymph node, intact liver, and perfused liver. Circulatory and resident cells were assessed via intravenous injection of a UV450 anti-CD45 antibody that labels circulatory cells exclusively followed by ex vivo labeling of resident cells using an AF700 anti-CD45 antibody.

(**D**) Frequency (left) and total immune cell count (right) from CyTOF data (as in Fig. 1D) in mice fed either the NCD or HFHC diet for 5 (n = 15 mice per group), 10 (n = 8 mice per group), or 15 weeks (n = 16 mice per group).

(**E**) Representative mass cytometry plots (left) and quantification (right) of IgM^+ IgD^+ B2 cells (n = 16 mice per group).

(**F**) Frequency of $TNF\alpha^+$ (middle) and $IL\text{-}6^+$ (right) B cells (as in Fig. 1G) after a 5-hr stimulation with PMA or the TLR agonists LPS (TLR4), ODN1826 (TLR9), and Pam3CSK4 (TLR1 and 2) in mice fed either an NCD or HFHC for 15 weeks (n = 12 mice per group).

(**G**) Frequency of $CD19^+$ $B220^+$ B cells, $CD11b^+$ $F4/80^+$ macrophages, and $CD11b^+$ $Ly6G^+$ gated from $CD45^+$ immune cells following immunomagnetic purification (n = 2 pooled mice per cell type).

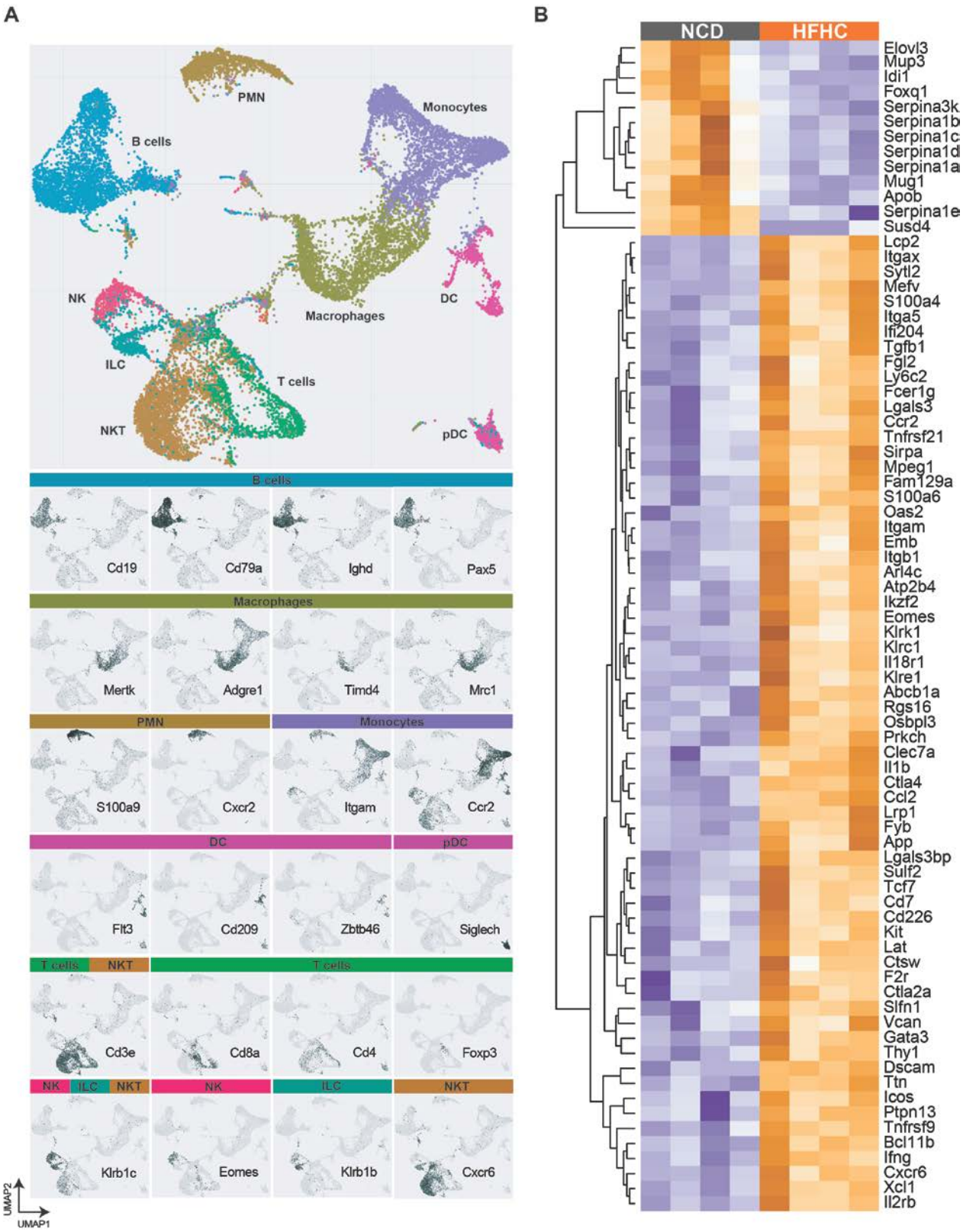

Supplementary Fig. 2 (Related to Fig. 2). Additional Data for single-cell and bulk RNA sequencing of immune cells and B cells from NCD and HFHC livers

(**A**) Immune cell subsets identified in intrahepatic immune cells using single-cell RNA sequencing (top) and UMAP projections of immune cells showing the expression of characteristic marker genes (bottom). Cells were isolated from the liver of NCD (n = 4) and HFHC (n = 5) mice.

(**B**) Hierarchical Heatmap of the Top Differentially Expressed Genes in B Cells from NASH Livers. B cells were purified from the liver of WT mice fed either an NCD or HFHC for 15 weeks and their gene expression was assessed by RNA-sequencing (n = 4 mice per group, FDR-corrected $P < 0.05$).

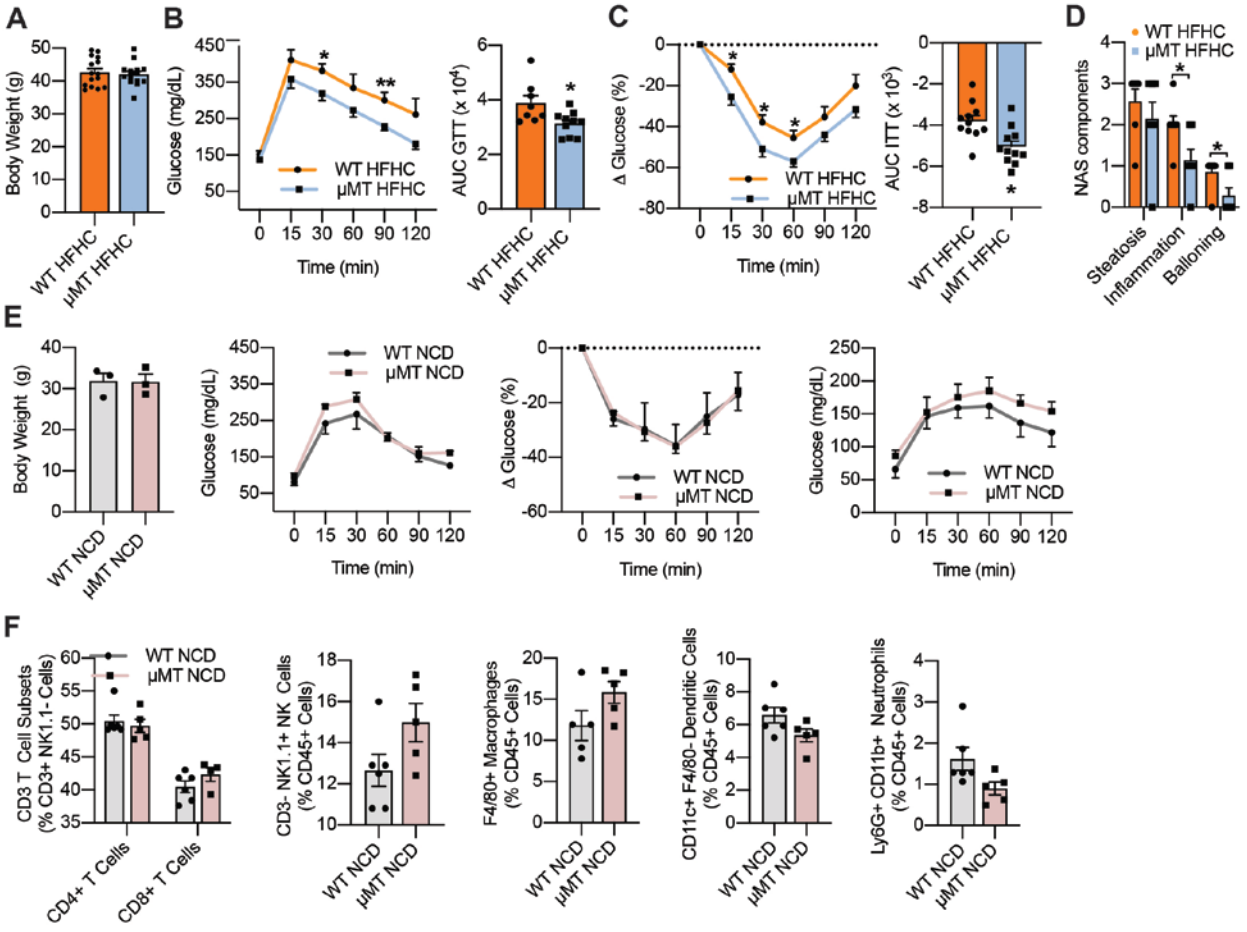

Supplementary Fig. 3 (Related to Fig. 3). Additional Data for NCD- and HFHC-fed µMT Mice

(**A**) Body weight (n = 15 mice per group).

(**B**) Glucose tolerance test (GTT, left) with corresponding areas under the curves (AUC, right; n = 8-10 mice per group) of WT and µMT mice fed the high-fat, high-carbohydrate (HFHC) diet for 15 weeks.

(**C**) Insulin tolerance test (ITT, left) with corresponding areas under the curves (AUC, right; n = 11-12 mice per group) of WT and µMT mice fed the HFHC diet for 15 weeks.

(**D**) NAS component scoring of H&E histology sections (n = 7 mice per group).

(**E**) Body-weight, GTT, ITT, and PTT of WT and µMT mice (n = 3 mice per group) fed a normal control diet (NCD) for 15 weeks.

(**F**) Frequency of intrahepatic T cells, NK cells, macrophages, dendritic cells, and neutrophils in WT and µMT mice (n = 3 mice per group) fed a NCD for 15 weeks.

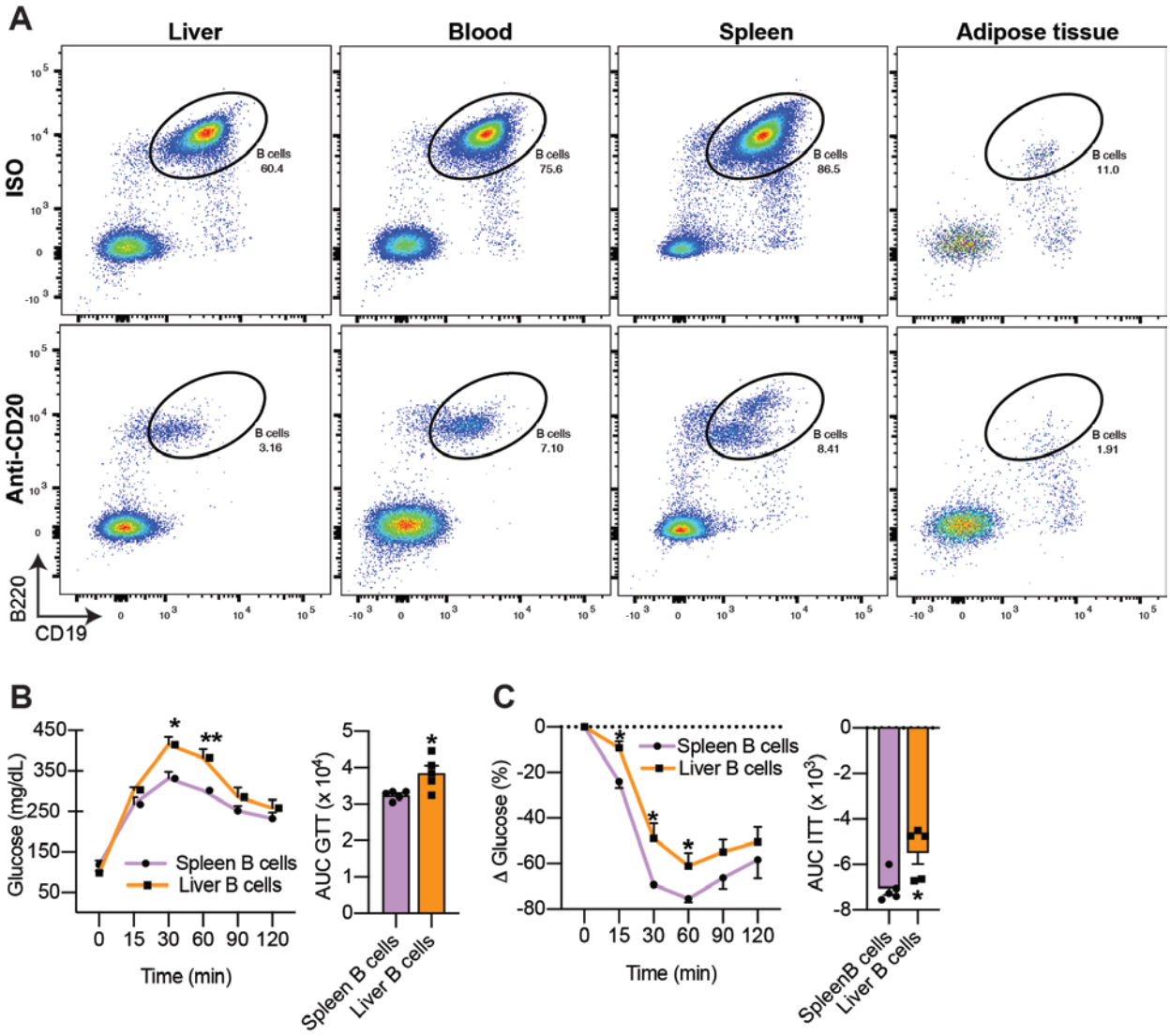

Supplementary Fig. 4 (Related to Fig. 4). Additional Data for CD20 mAb and Metabolic Data for Adoptive Transfer Experiment

(**A**) Representative flow cytometry plots showing $CD19^+$ $B220^+$ B cells in the liver, blood, spleen, and adipose tissue of WT mice 3 weeks after injection of a single dose of 250 mg anti-CD20 antibody (CD20 mAb, n = 3 mice).

(**B-C**) B cells (1×10^6) were purified from either the spleen or liver of WT donor mice fed the HFHC diet for 15 weeks and adoptively transfer via intraperitoneal injection into μMT recipient mice fed the HFHC diet for 11 weeks. Experiments were performed 4 weeks after adoptive transfer.

(**B**) Glucose tolerance test (GTT, left) with corresponding areas under the curves (AUC, right; n = 5 mice per group).

(**C**) Insulin tolerance test (ITT, left) with corresponding areas under the curves (AUC, right; n = 5 mice per group).

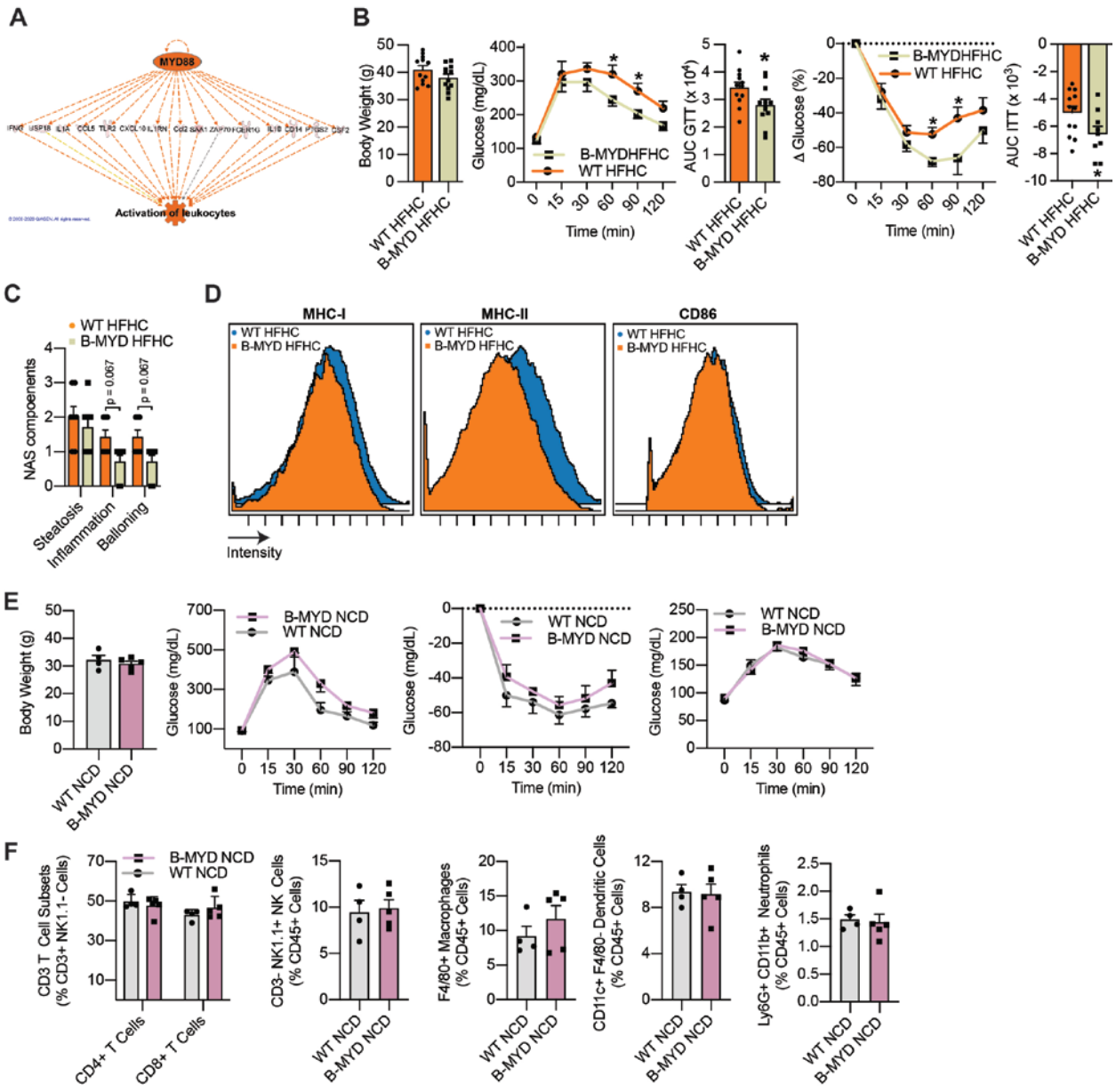

Supplementary Fig. 5 (Related to Fig. 5). Additional Data for NCD- and HFHC-fed B-MYD mice

(**A**) Upstream Regulator Analysis of MyD88 generated from Ingenuity Pathway Analysis (IPA) from Fig. 2. Used with permission from QIAGEN.

(**B**) Body weight (left, n = 12 mice per group), glucose tolerance test (GTT, middle) with corresponding areas under the curves (AUC, right; n = 12 mice per group), and insulin tolerance test (ITT, right) with corresponding areas under the curves (AUC, right; n = 12 mice per group).

(**C**) NAS component scoring of H&E histology sections (n = 7 mice per group).

(**D**) Representative CyTOF histograms of mean intensity showing the B cell expression of MHC-I (left), MHC-II (middle), and CD86 (right) in mice HFHC B-MYD mice (as in Fig. 5H).

(**E**) Body-weight, glucose tolerance test, insulin tolerance test, and pyruvate tolerance test of WT and B-MYD mice (n = 4-5 mice per group) fed a normal control diet (NCD) for 15 weeks.

(**F**) Frequency of intrahepatic T cells, NK cells, macrophages, dendritic cells, and neutrophils in WT and B-MYD mice (n = 4-5 mice per group) fed a NCD for 15 weeks.

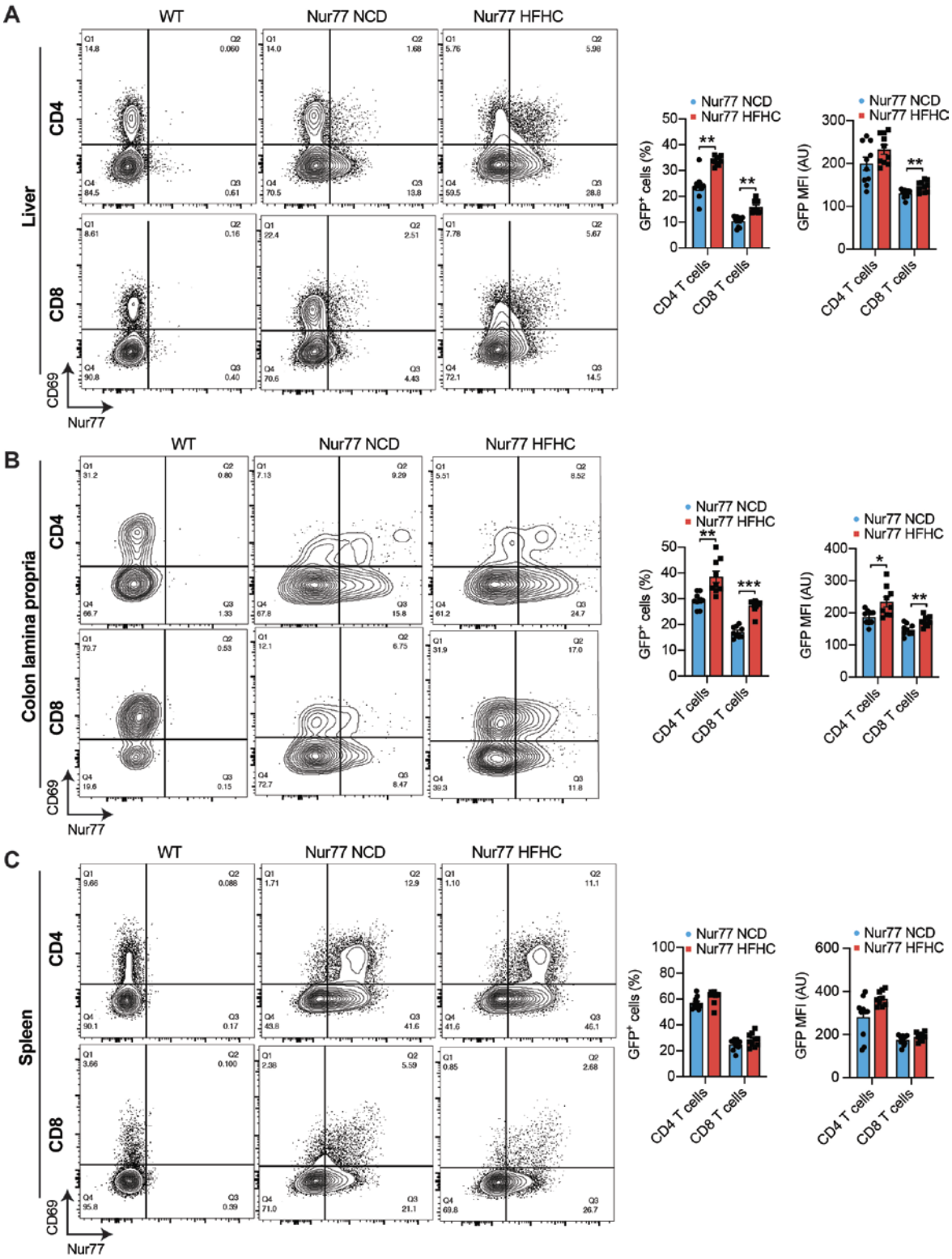

Supplementary Fig. 6 (Related to Fig. 6). Additional Data for Nur77-GFP mice

(**A**) Representative flow cytometry plots (left) and quantification (right) of intrahepatic GFP$^+$ CD69$^-$ CD4 and CD8 T cells (n = 10 mice per group).

(**B**) Representative flow cytometry plots (left) and quantification (right) of colon lamina propria GFP^+ $CD69^-$ CD4 and CD8 T cells (n = 10 mice per group).

(**C**) Representative flow cytometry plots (left) and quantification (right) of splenic GFP^+ $CD69^-$ CD4 and CD8 T cells (n = 10 mice per group).

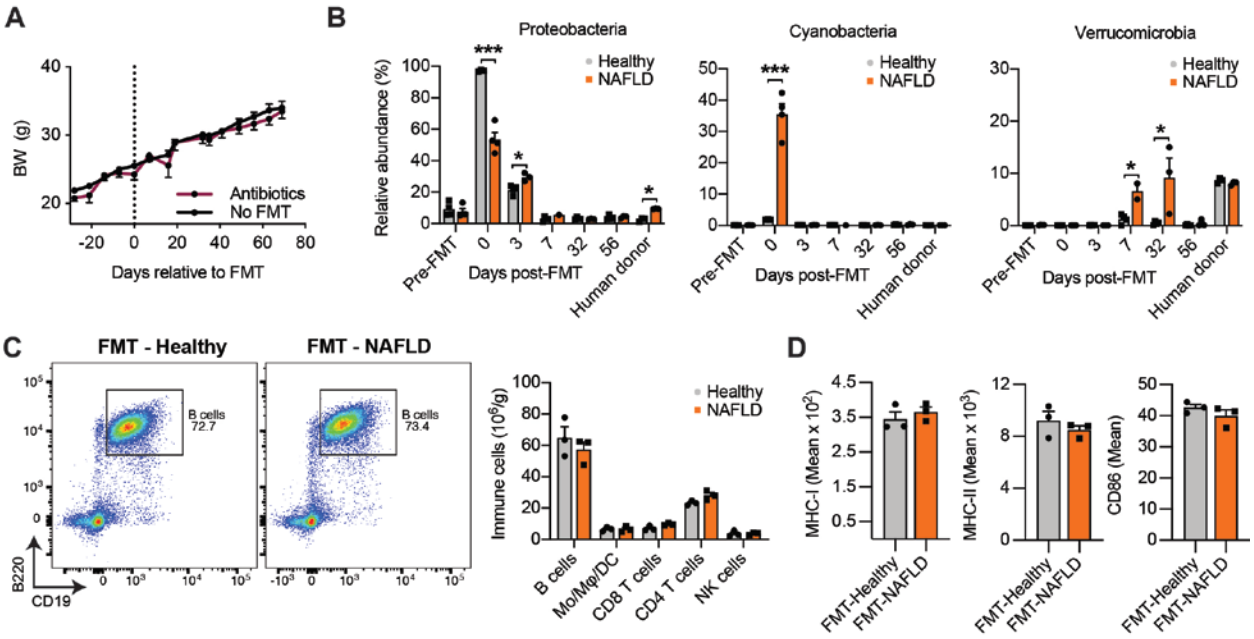

Supplementary Fig. 7 (Related to Fig. 7). Additional Data for Fecal Microbiota Transplantation Experiments

(**A**) Body weight of WT mice fed a normal control diet (NCD) that were left untreated (No FMT) or received antibiotics in the drinking water for 21 days but did not receive an FMT (n = 7-8 mice per group).

(**B**) Abundance of *Proteobacteria* (left), *Cyanobacteria* (middle), and *Verrucomicrobia* (right) in fecal communities of human donors (1 healthy and 1 NAFLD patient) and recipient mice at different timepoints relative to the FMT (n = 3-4 mice per group).

(**C**) Representative flow cytometry plot showing CD19+ B220+ B cells (left) and number (right) of splenic B cells, monocytes (Mo), macrophages (Mφ), dendritic cells (DC), CD4 and CD8 T cells, and natural killer (NK) cells (right, n = 6-7 mice per group) in recipient mice 10 weeks post-FMT.

(**D**) Mean intensity of splenic B cell expression of MHC-I (left), MHC-II (middle), and CD86 (right, n = 4 mice per group) in recipient mice 10 weeks post-FMT.

Supplementary Table 1. qRT-PCR Primer Sequences

Primer	Sequence	Source
Actb	Forward: 5′-TGTTACCAACTGGGACGACA-3′ Reverse: 5′-CTTTTCACGGTTGGCCTTAG-3′	Integrated DNA Technologies
Gapdh	Forward: 5′-AACGACCCCTTCATTGAC-3′ Reverse: 5′-TCCACGACATACTCAGCAC-3′	Integrated DNA Technologies
Acta2	Forward: 5′-GGCTCTGGGCTCTGTAAGG-3′ Reverse: 5′-CTCTTGCTCTGGGCTTCATC-3′	Integrated DNA Technologies
Col1a1	Forward: 5′-ACATGTTCAGCTTTGTGGACC-3′ Reverse: 5′-TAGGCCATTGTGTATGCAGC-3′	Integrated DNA Technologies
Tgfb1	Forward: 5′-GGTTCATGTCATGGATGGTGC-3′ Reverse: 5′-TGACGTCACTGGAGTTGTACGG-3′	Integrated DNA Technologies
Mmp2	Forward: 5′-TTCCCCCGCAAGCCCAAGTG-3′ Reverse: 5′-GAGAAAAGCGCAGCGGAGTGACG-3′	Integrated DNA Technologies
Timp1	Forward: 5′-GCATCTCTGGCATCTGGCATC-3′ Reverse: 5′-GCGGTTCTGGGACTTGTGGGC-3′	Integrated DNA Technologies
Tnfa	Forward: 5′-GTAGCCCACGTCGTAGCAAAC-3′ Reverse: 5′-AGTTGGTTGTCTTTGAGATCCATG-3′	Integrated DNA Technologies
Icam1	Forward: 5′-CGTGTGCCATGCCTTTAGCT-3′ Reverse: 5′-TCCAGTTATTTTGAGAGTGGTACAGTACTG-3′	Integrated DNA Technologies
Sele	Forward: 5′-AGATACTTTCGGAAGAAAGCAAAGAA-3′ Reverse: 5′-GTAAGAAGGCACATGGTAGTTTTCAA-3′	Integrated DNA Technologies
Inos	Forward: 5′-CCGAAGCAAACATCACATTCA-3′ Reverse: 5′-GGTCTAAAGGCTCCGGGCT-3′	Integrated DNA Technologies
Il1b	Forward: 5′-ACCCTGCAGCTGGAGAGTGT-3′ Reverse: 5′-TTGACTTCTATCTGTTGAAGACAAACC-3′	Integrated DNA Technologies

Actb, Beta-actin; *Gapdh*, glyceraldehyde-3-phosphate dehydrogenase; *Acta2*, actin alpha 2, smooth muscle; *Col1a1*, collagen type I alpha 1; Tgfb1, transforming growth factor, beta; *Mmp2*, matrix metallopeptidase 2; *Tnfa*, tumor necrosis factor-alpha; *Icam1*, intercellular adhesion molecule 1; *Sele*, e-selectin; *Inos*, nitric oxide synthase 2, inducible; *Il1b*, interleukin 1 beta.

Supplementary Table 2. Human Microbiota Donor Information

Donor	Group	BMI	ALT (U/L)	AST (U/L)	ALK P (U/L)	Origen
Lean	Healthy	< 85th percentile	NA	NA	NA	Minnesota Microbiota Therapeutics Donor Program
NAFLD A	Obese/NAFLD	NA	504	291	155	Minnesota Microbiota Therapeutics Donor Program
NAFLD B	Obese/NAFLD	34.8	75	25	69	Cincinnati Children's Hospital
NAFLD C	Obese/NAFLD	30.58	135	55	295	Cincinnati Children's Hospital

Supplementary Table 3. Differentially Expressed Genes between NCD and HFHC B cells from the Single-Cell RNA-Sequencing Analysis

Gene	Avg_logFC	P_val_adj	Pct.1	Pct.2	P_val
S100a9	12.20854356	0.000990961	0.504	0.419	3.30E-07
S100a8	11.3329318	0.002149947	0.48	0.429	7.17E-07
Slpi	11.08925063	0.008439727	0.389	0.333	2.81E-06
Cxcl2	10.90959291	0.002127303	0.359	0.296	7.09E-07
Cxcr4	9.850594178	2.56E-05	0.433	0.358	8.54E-09
Trem1	8.471630098	0.038061751	0.41	0.34	1.27E-05
Il1b	5.963938441	4.32E-05	0.385	0.318	1.44E-08
G0s2	4.461795323	0.023162173	0.457	0.383	7.72E-06
Btla	4.333383455	0.043688212	0.544	0.502	1.46E-05
Gm8369	3.95185176	2.62E-08	0.484	0.379	8.74E-12
mt-Cytb	3.777380286	0.043707067	0.667	0.616	1.46E-05
Pgap1	3.746169031	0.000709674	0.517	0.428	2.37E-07
Hdc	3.603389294	0.000255986	0.428	0.361	8.53E-08
Trim34a	3.211456867	0.004099007	0.426	0.358	1.37E-06
H2-Ab1	3.074635785	0.000126462	0.737	0.64	4.22E-08
Hist1h1d	1.68507578	0.000182349	0.256	0.191	6.08E-08
Jam2	1.662550927	0.013892724	0.28	0.209	4.63E-06
Man1a	1.619313335	0.045707981	0.548	0.492	1.52E-05
Ehd3	1.473283872	0.000135028	0.267	0.213	4.50E-08
Stk17b	1.448220836	5.69E-10	0.693	0.623	1.90E-13
Gimap6	1.378067447	5.41E-05	0.569	0.492	1.80E-08
Meis2	1.362078578	0.010870335	0.302	0.236	3.62E-06
Cd74	1.310117008	4.29E-05	0.92	0.883	1.43E-08
Stap1	1.190943337	0.006954336	0.528	0.445	2.32E-06
H2-Eb1	1.188566958	0.000162873	0.708	0.606	5.43E-08
Bmp2	1.087868672	0.003548942	0.257	0.202	1.18E-06
Folr2	0.957113297	0.007911914	0.253	0.191	2.64E-06
Abca1	0.942403007	7.15E-15	0.317	0.211	2.38E-18
Ighd	0.869190655	1.06E-07	0.808	0.719	3.54E-11
Cd33	0.824619097	0.02050278	0.334	0.246	6.83E-06
Zfp36l1	0.798086881	4.17E-06	0.695	0.629	1.39E-09
Gas6	0.761528329	0.003713727	0.288	0.209	1.24E-06
Fcer2a	0.674065567	0.002662384	0.602	0.518	8.87E-07
Rasgrp3	0.58327776	0.000276438	0.368	0.276	9.21E-08
Aass	0.550130127	0.024076902	0.27	0.202	8.03E-06
Fcgr2b	0.475690416	0.010696229	0.322	0.28	3.57E-06
Adgrf5	0.430478093	0.003420783	0.296	0.232	1.14E-06

Dnase1l3	0.390082083	0.00431747	0.285	0.247	1.44E-06
Fam124a	0.371969274	0.004935294	0.274	0.198	1.65E-06
H2-Aa	0.299605547	3.80E-05	0.756	0.663	1.27E-08
Ltbp4	0.297145584	0.01722026	0.269	0.204	5.74E-06
Srgn	0.294223888	0.000845303	0.45	0.389	2.82E-07
Fermt2	0.285786193	0.008722634	0.255	0.185	2.91E-06
Mylip	0.278223957	0.003074858	0.374	0.296	1.02E-06
Clec4d	0.253856052	9.13E-06	0.411	0.334	3.04E-09
Eng	-0.262662717	0.020237231	0.253	0.195	6.75E-06
Ighm	-0.27131598	0.000641266	0.956	0.943	2.14E-07
Cd24a	-0.317997804	9.43E-08	0.525	0.591	3.14E-11
Vpreb3	-0.369656798	1.23E-06	0.444	0.512	4.09E-10
Clec4f	-0.416229265	0.020080716	0.375	0.31	6.69E-06
Ly6d	-0.501820103	0.000540827	0.811	0.827	1.80E-07
Iglc1	-0.512507395	7.64E-06	0.484	0.548	2.55E-09
Gpr182	-0.545029462	0.00049368	0.274	0.219	1.65E-07
Spib	-0.560325483	0.000169315	0.467	0.542	5.64E-08
Hspa1b	-0.561846675	0.000779261	0.312	0.38	2.60E-07
Zfp36	-0.631291995	1.54E-05	0.484	0.404	5.14E-09
Fam129c	-0.728015981	0.000583259	0.285	0.341	1.94E-07
Ms4a1	-0.756295985	1.53E-06	0.849	0.853	5.09E-10
Tnfrsf13c	-0.7777648	0.033396229	0.515	0.574	1.11E-05
Hspa1a	-1.127398296	9.33E-06	0.237	0.308	3.11E-09
Tsc22d3	-1.251524904	5.97E-12	0.748	0.653	1.99E-15
Rasgrp1	-1.418143464	0.002346099	0.254	0.313	7.82E-07
Dnajb1	-1.634417282	0.001235415	0.303	0.374	4.12E-07

Supplementary Table 4. Reagents and Resources

REAGENT or RESOURCE	SOURCE	IDENTIFIER
Antibodies		
Rat anti-mouse I-A/I-E-174Yb (M5/114.15.2)	Fluidigm	Cat #: 3174003B
Rat anti-mouse CD11b-148Nd (M1/70)	Fluidigm	Cat #: 3148003B
Rat anti-mouse F4/80-159Tb (BM8)	Fluidigm	Cat #: 3159009B
Rat anti-mouse Ly-6G-141Pr (1A8)	Fluidigm	Cat #: 3141008B
Hamster anti-mouse CD3e-152Sm (145-2C11)	Fluidigm	Cat #: 3152004B
Rat anti-mouse CD62L-160Gd (MEL-14)	Fluidigm	Cat #: 3160008B
Rat anti-mouse CD44-169Tm (IM7)	Biolegend (antibody) Fluidigm (metal)	Cat #: 103002 Cat #: 201300
Mouse anti-mouse MHC Class I-144Nd (28-14-8)	Fluidigm	Cat #: 3144016B
Rat anti-mouse CD4-145Nd (RM4-5)	Fluidigm	Cat #: 3145002B
Hamster anti-mouse CD11c-142Nd (N418)	Fluidigm	Cat #: 3142003B
Rat anti-mouse CD19-149Sm (6D5)	Fluidigm	Cat #: 3149002B
Rat anti-mouse CD8a-168Er (53-6.7)	Fluidigm	Cat #: 3168003B
Mouse anti-mouse NK1.1-170Er (PK136)	Fluidigm	Cat #: 3170002B
Rat anti-mouse CD86-172Yb (GL1))	Fluidigm	Cat #: 3172016B
Rat anti-mouse CD45R/B220-176Yb (RA3-6B2)	Biolegend (antibody) Fluidigm (metal)	Cat #: 103249 Cat #: 201300
Mouse anti-mouse CD45.2-147Sm (104)	Fluidigm	Cat #: 3147004B
Rat anti-mouse IgD-156Gd (11-26c.2a)	Biolegend (antibody) Fluidigm (metal)	Cat #: 405737 Cat #: 201300
Rat anti-mouse IgM-151Eu (RMM-1)	Fluidigm	Cat #: 3151006B
Rat anti-mouse CD5-146Nd (53-7.3)	Fluidigm	Cat #: 3146012B
Rat anti-mouse TNFα-162Dy (MP6-XT22)	Fluidigm	Cat #: 3162002B
Rat anti-mouse IFNγ-166Er (XMG1.2)	Biolegend (antibody) Fluidigm (metal)	Cat #: 505843 Cat #: 201166
Rat anti-mouse IL-6-167Er (MP5-20F3)	Fluidigm	Cat #: 31670003B
Mouse anti-mouse CD45.2-AF700 (104)	Biolegend	Cat #: 109822
Mouse anti-mouse CD45.2-V450 (104)	BD Bioscience	Cat #: 560697
Hamster anti-mouse CD3e-BUV737 (145-2C11)	BD Bioscience	Cat #: 612771

Rat anti-mouse CD4-BUV395 (RM4-5)	BD Bioscience	Cat #: 740208
Rat anti-mouse CD8a-BUV805 (53-6.7)	BD Bioscience	Cat #: 564920
Rat anti-mouse CD11b-PE/Cy7 (M1/70)	Biolegend	Cat #: 101216
Rat anti-mouse CD19-BV785 (6D5)	Biolegend	Cat #: 115543
Rat anti-mouse CD45R/B220-BV421 (RA3-6B2)	Biolegend	Cat #: 103251
Mouse anti-mouse NK1.1-APC (PK136)	Biolegend	Cat #: 108709
Hamster anti-mouse CD11c-BV711 (N418)	Biolegend	Cat #: 117349
Rat anti-mouse Ly-6G-PE (1A8)	Biolegend	Cat #: 127607
Rat anti-mouse F4/80-FITC (BM8)	Biolegend	Cat #: 123108
Rat anti-mouse F4/80-AF594 (BM8)	Biolegend	Cat #: 123140
Rat anti-mouse IFNγ-PE (XMG1.2)	Biolegend	Cat #: 505807
Rat anti-mouse TNFα-BV650 (MP6-XT22)	Biolegend	Cat #: 506333
Rat anti-mouse IL-2-AF488 (JES6-5H4)	Biolegend	Cat #: 503813
Rat anti-mouse IL-6-PerCP-eFluor 710 (MP5-20F3)	ThermoFisher	Cat #: 46706180
Rat anti-mouse CD44-BV711 (IM7)	Biolegend	Cat #: 103057
Rat anti-mouse CD62L-BV606 (GL-3)	Biolegend	Cat #: 104437
Rat anti-mouse CD86-PE (GL-1)	Biolegend	Cat #: 105007
Rat anti-mouse I-A/I-E-FITC (M5/114.15.2)	Biolegend	Cat #: 107605
Rat anti-mouse IL-6-PE (MP5-20F3)	Biolegend	Cat #: 504503
Rat anti-mouse IFNγ-BV711 (XMG1.2)	BD Bioscience	Cat #: 564336
Rat anti-mouse CD44-PE (IM7)	Biolegend	Cat #: 103008
Hamster anti-mouse CD11c-APC/Cy7 (N418)	Biolegend	Cat #: 117323
Hamster anti-mouse CD69-BV421 (H1.2F3)	Biolegend	Cat #: 104527
Rat anti-mouse CD16/32 (93)	Biolegend	Cat #: 101320
Mouse anti-mouse CD20 (5D2)	Yinjie Chen, U. of Mississippi	N/A
GP120 isotype control	Yinjie Chen, U. of Mississippi	N/A
Mouse anti-human CD19 (clone LE-CD19)	ThermoFisher	Cat #: MA1-81724

Biological Samples		
Human liver biopsies from NAFLD patients	Ghazarian et al. 2017	N/A
Chemicals, Peptides, and Recombinant Proteins		
Cell stimulation cocktail + protein transport inhibitor	ThermoFisher	Cat #: 00497593
LPS	ThermoFisher	Cat #: 00497093
Protein transport inhibitor	ThermoFisher	Cat #: 00498003
Pam3CSK4	Invivogen	Cat #: tlr1-kit1mw
ODN1826	Invivogen	Cat #: tlr1-kit1mw
Cell-ID Cisplatin	Fluidigm	Cat #: 201194
Cell-ID Intercalator-Ir	Fluidigm	Cat #: 201192B
Pierce 16% Formaldehyde	ThermoFisher	Cat #: 28906
Zombie Agua fixable viability kit	Biolegend	Cat #: 423102
Maxpar X8 multimetal labeling kit	Fluidigm	Cat #: 201300
Critical Commercial Assays		
BD Cytofix/Cytoperm kit	BD Bioscience	Cat #: 554714
ELISA Max Deluxe set mouse TNFα	Biolegend	Cat #: 430904
ELISA Max Deluxe set mouse IL-6	Biolegend	Cat #: 431304
RNeasy Plus Mini kit	Qiagen	Cat #: 74136
RNeasy MinElute cleanup kit	Qiagen	Cat #: 74204
iScript cDNA Synthesis kit	Bio-Rad	Cat #: 1708890
SYBR Green Supermix	Bio-Rad	Cat #: 1708882
Experimental Models: Organisms/Strains		
Mouse: C57BL/6J	The Jackson Laboratory	Cat #; 000664
Mouse: µMt (B6.129S2-Ighm^{tm1Cgn}/J)	The Jackson Laboratory	Cat #: 002288
Mouse: CD19^{cre} (B6.129P2(C)-CD19$^{tm1(cre)Cgn}$/J)	The Jackson Laboratory	Cat #: 006785
Mouse: Myd88$^{fl/fl}$ (B6.129P2(SJL)-Myd88^{tm1Defr}/J)	The Jackson Laboratory	Cat #: 008888
Mouse: HEL (C57BL/6-Tg(IghelMD4)4Ccg/J)	The Jackson Laboratory	Cat #: 002595

Mouse Nur77^{GFP} (C57BL/6-Tg(Nr4a1-EGFP/cre)820Khog/J)	The Jackson Laboratory	Cat #: 016617
Oligonucleotides		
Primers for qRT-PCR, See Table S1	This paper	N/A
Software and Algorithms		
FIJI	ImageJ	imagej.net/Fiji
Prism 8.3	GraphPad	Version 8
edgeR	Bioconductor	Version 3
Ingenuity Pathway Analysis	Qiagen	N/A

REFERENCES

1. Revelo XS, Tsai S, Lei H, Luck H, Ghazarian M, Tsui H, Shi SY, et al. Perforin is a novel immune regulator of obesity-related insulin resistance. Diabetes 2015;64:90-103.
2. Ghazarian M, Revelo XS, Nohr MK, Luck H, Zeng K, Lei H, Tsai S, et al. Type I Interferon Responses Drive Intrahepatic T cells to Promote Metabolic Syndrome. Sci Immunol 2017;2.
3. Revelo XS, Ghazarian M, Chng MH, Luck H, Kim JH, Zeng K, Shi SY, et al. Nucleic Acid-Targeting Pathways Promote Inflammation in Obesity-Related Insulin Resistance. Cell Rep 2016;16:717-730.
4. Hafemeister C, Satija R. Normalization and variance stabilization of single-cell RNA-seq data using regularized negative binomial regression. Genome Biol 2019;20:296.
5. Becht E, McInnes L, Healy J, Dutertre CA, Kwok IWH, Ng LG, Ginhoux F, et al. Dimensionality reduction for visualizing single-cell data using UMAP. Nat Biotechnol 2018.
6. Aran D, Looney AP, Liu L, Wu E, Fong V, Hsu A, Chak S, et al. Reference-based analysis of lung single-cell sequencing reveals a transitional profibrotic macrophage. Nat Immunol 2019;20:163-172.
7. Linares-Cervantes I, Echeverri J, Cleland S, Kaths JM, Rosales R, Goto T, Kollmann D, et al. Predictor parameters of liver viability during porcine normothermic ex situ liver perfusion in a model of liver transplantation with marginal grafts. Am J Transplant 2019;19:2991-3005.
8. Staley C, Kaiser T, Beura LK, Hamilton MJ, Weingarden AR, Bobr A, Kang J, et al. Stable engraftment of human microbiota into mice with a single oral gavage following antibiotic conditioning. Microbiome 2017;5:87.
9. Brunt EM, Kleiner DE, Wilson LA, Belt P, Neuschwander-Tetri BA, (CRN) NCRN. Nonalcoholic fatty liver disease (NAFLD) activity score and the histopathologic diagnosis in NAFLD: distinct clinicopathologic meanings. Hepatology 2011;53:810-820.

10. Bruzzi S, Sutti S, Giudici G, Burlone ME, Ramavath NN, Toscani A, Bozzola C, et al. B2-Lymphocyte responses to oxidative stress-derived antigens contribute to the evolution of nonalcoholic fatty liver disease (NAFLD). Free Radic Biol Med 2018;124:249-259.